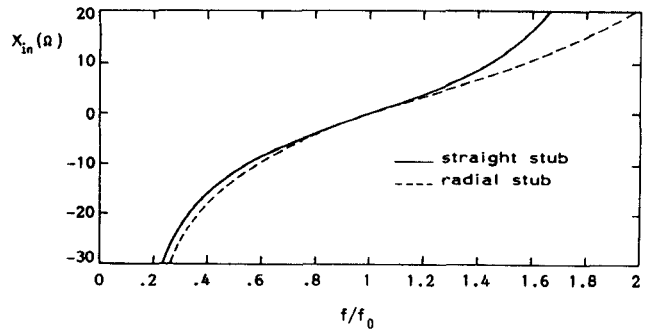

Fig. 6. Computed behaviors of input reactance of a radial stub with $\alpha = 120°$ (----) and a straight stub (——) having the same slope parameter and the same frequency f_0.

well as of the scattering parameters of shunt stubs are in very good agreement with theoretical results. The characterization of the radial stub in terms of an equivalent characteristic impedance has shown the suitability of such a structure as an alternative to the conventional straight stub, as it exhibits a very low characteristic impedance and allows an accurate localization of the impedance reference plane.

ACKNOWLEDGMENT

Prof. T. Itoh is acknowledged for helpful discussions and suggestions.

REFERENCES

[1] J. P. Vinding, "Radial line stubs as elements in strip line circuits," in *NEREM Record*, 1967, pp. 108–109.
[2] A. H. Atwater, "Microstrip reactive circuit elements," *IEEE Trans. Microwave Theory Tech.*, vol. MTT-31, pp. 488–491, June 1983.
[3] G. D'Inzeo, F. Giannini, C. M. Sodi, and R. Sorrentino, "Method of analysis and filtering properties of microwave planar networks," *IEEE Trans. Microwave Theory Tech.*, vol. MTT-26, pp. 462–471, July 1978.
[4] G. D'Inzeo, F. Giannini, R. Sorrentino, and J. Vrba, "Microwave planar networks: The annular structure," *Electron. Lett.*, vol. 14, no. 16, pp. 526–528, Aug. 1978.
[5] J. Vrba, "Dynamic permittivities of microstrip ring resonators," *Electron. Lett.*, vol. 15, no. 16, pp. 504–505, Aug. 1979.
[6] I. Wolff and N. Knoppik, "Rectangular and circular microstrip disk capacitors and resonators," *IEEE Trans. Microwave Theory Tech.*, vol. MTT-22, pp. 857–864, Oct. 1974.
[7] K. C. Gupta, Ramesh Garg, and I. J. Bahl, *Microstrip Lines and Slotlines*. Dedham: Artech House, 1979, chap. 2.
[8] A. H. Atwater, private communication.

Broad-Band Millimeter-Wave *E*-Plane Bandpass Filters

L. Q. BUI, D. BALL, MEMBER, IEEE, AND T. ITOH, FELLOW, IEEE

Abstract—**An accurate method to obtain starting estimates for an *E*-plane bandpass filter CAD program recently developed by Shih, Itoh, and Bui is presented. Results agree very well with exact values for filter design with relative bandwidths exceeding 10 percent at *W*-band and *D*-band and 20 percent at lower frequencies.**

I. INTRODUCTION

WITH INCREASING activity in millimeter-wave integrated circuit development, the *E*-plane filter shown in Fig. 1 recently has drawn considerable attention [1]–[5]. Such a structure consists of metal strips inserted along the *E*-plane of a rectangular waveguide. The strips may be fabricated on dielectric substrates [3]–[5], in which case this filter is quite compatible with finline technology.

To date, many *E*-plane filter designs reported are limited to narrow bandwidths of less than a few percent. For wide-band designs, as all the resonators are strongly coupled, an accurate analysis procedure, one which takes into account the interaction not only of the dominant mode but also of the higher order modes generated at the edge of the strips, is necessary.

We recently developed a computerized (CAD) algorithm for a class of *E*-plane filters [6]. For narrow-band designs, the algorithm converges rapidly with the prescribed response by use of available optimization routines [7]. However, since no systematic scheme was incorporated for providing starting values of the optimization routine, convergence of the CAD program was rather slow; furthermore, the cost of generating acceptable design parameters often was prohibitively expensive. This deficiency is especially noticeable in design of relative bandwidth greater than 5 percent. Since *E*-plane filters are inductively direct-coupled cavity filters, the conventional design procedure given by Levy using an impedance inverter and low-pass prototypes is available as [8]. Depending on the bandwidth equipment, either a lumped-element or a distributed prototype is used to calculate the inverter values. In general, a distributed prototype is not favorable due to difficulties in

Manuscript received April 26, 1984; revised August 1, 1984.

L. Q. Bui and D. Ball are with the Hughes Aircraft Company, Microwave Products Division, Torrence, CA 90509.

T. Itoh is with the Department of Electrical Engineering, the University of Texas at Austin, Austin, TX 78712.

0018-9480/84/1200-1655$01.00 ©1984 IEEE

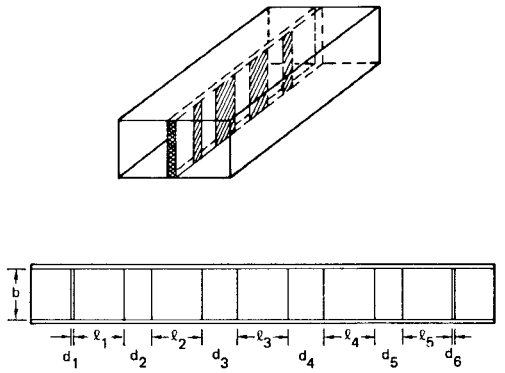

Fig. 1. *E*-plane filter structure.

obtaining either impedance values using network synthesis technique or element values for untabulated design, even if such prototype can be used for wide-band design [9].

This paper presents an accurate method that uses an explicit formula to obtain the element values of a distributed low-pass prototype element derived by Rhodes [10]. The equivalent circuit of an *E*-plane inductive strip [6] is used to obtain design parameters such as septum widths and spacing. Results agree with exact values for filter designs of up to 30-percent bandwidth extremely well. The computation cost was reduced substantially since no optimization is required. Using this modified CAD program, designs of *E*-plane bandpass filters with more than 10-percent bandwidth at *D*-band and *W*-bands and more than 20 percent at lower frequency ranges have been accomplished. Results are unprecedented to our best knowledge.

II. Procedures

As described in [6], our original CAD program consists of one optimization routine and one analysis algorithm. The analysis consists of three steps. In the first step, the generalized scattering matrix at a strip edge is calculated. For instance, $S_{11}(m, p)$ is the amplitude of the reflected mth mode when the pth mode is incident on that edge. Because each strip extends from the lower broad wall to the upper broad wall of the waveguide and is uniform, these generalized scattering parameters can be calculated exactly by residue calculus techniques [11]. The second step computes the generalized S matrix of a strip by combining the S parameters derived in step 1 for both edges of the strip. The last step combines generalized S matrices of several strips. This algorithm allows us to obtain the generalized S matrix of the entire filter structure (Fig. 1). Note that the use of the generalized S matrix enables us to find the interactions between junctions due to the dominant mode and to all higher order modes. This is quite important for accurate design of wide-band filters. The effect of higher order mode interactions becomes even more important for filters in which the strips are narrow and the resonators are coupled strongly.

The procedure is based on a formulation proposed by Rhodes for a distributed stepped-impedance low-pass prototype [10]. When the passband ripple ϵ, the lower and upper frequencies f_L and f_H, and the out-of-band rejection L (decibels) are specified, the procedure is as follows.

1) Determine the midband guide wavelength λ_{go} by solving

$$\lambda_{gL}\sin(\pi\lambda_{go}/\lambda_{gL})+\lambda_{gH}\sin(\pi\lambda_{go}/\lambda_{gH})=0 \quad (1)$$

where λ_{gL} and λ_{gH} are the guide wavelengths in the resonator section at f_L and f_H. For a narrow-band case ($\lambda_{gL}\approx\lambda_{gH}$)

$$\lambda_{go}=\frac{\lambda_{gL}+\lambda_{gH}}{2}.$$

However, for the broad-band case, (1) generally must be solved numerically.

2) Determine the scaling parameter α by

$$\alpha=\lambda_{go}/\left[\lambda_g\sin(\pi\lambda_{go}/\lambda_{gL})\right]. \quad (2)$$

3) Determine the number of resonators N. This is accomplished by finding the minimum value of N for which the most severe constraints on the rejection L satisfies

$$L=10\log\left\{1+\epsilon^2T_N^2\left[\alpha\frac{\lambda_g}{\lambda_{go}}\sin\left(\frac{\pi\lambda_{go}}{\lambda_g}\right)\right]\right\} \quad (3)$$

at the designated stopband frequency f_s. In (3), T_N is the Chebyshev polynomial of degree N, and λ_g is the guide wavelength at f_s.

4) Calculate the impedances of the distributed element and impedance inverter values

$$Z_n=2\alpha\sin\left[\frac{(2n-1)\pi}{2N}\right]\Big/y - \frac{1}{4y\alpha}\left\{\frac{y^2+\sin^2(n\pi/N)}{\sin\frac{(2n+1)\pi}{2N}} + \frac{y^2+\sin^2[(n-1)\pi/N]}{\sin\frac{(2n-3)\pi}{2N}}\right\}, \qquad n=1,\cdots,N \quad (4)$$

$$k'_{n,n+1}=\frac{\sqrt{y^2+\sin^2(n\pi/N)}}{y}, \qquad n=0,1,\cdots,N \quad (5)$$

where

$$y=\sinh\left[\frac{1}{N}\sinh^{-1}\frac{1}{\epsilon}\right]. \quad (6)$$

5) Recognizing that the characteristic impedances of the resonator sections are identical, scale the impedance Z_n to unity and

$$K_{n,n+1}=k'_{n,n+1}/\sqrt{Z_nZ_{n+1}}, \qquad n=0,\cdots,N \quad (7)$$

and

$$Z_0=Z_{n+1}=1.$$

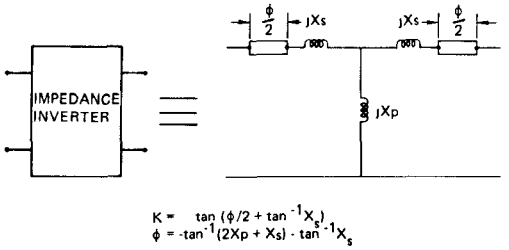

Fig. 2. Impedance inverter.

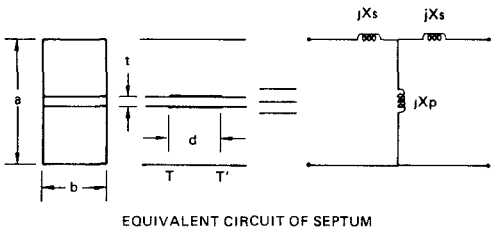

Fig. 3. Equivalent circuit of a bilateral fin.

6) Determine the widths of E-plane strips so that the required impedance inverter is realized. Use the T equivalent circuit of the strip for the inverter (Fig. 2)

$$K = \left| \tan\left(\frac{\phi}{2} + \tan^{-1} X_s\right)\right| \tag{8}$$

$$\phi = -\tan^{-1}(2X_p + X_s) - \tan^{-1} X_s. \tag{9}$$

The normalized reactances X_p and X_s in Fig. 3 are given in [10]

$$jX_s = \frac{1 - S_{12} + S_{11}}{1 - S_{11} + S_{12}} \tag{10a}$$

$$jX_p = \frac{2S_{12}}{(1 - S_{11})^2 - S_{11}^2} \tag{10b}$$

where S_{11}, etc., are the scattering coefficients of the dominant mode. Note that, in calculating X_s and X_p, effects of all of the higher order modes are incorporated. Therefore, the results are accurate.

X_s and X_p in (10) are functions of the strip width d as described in [6]. Since these functions are not available explicitly, we implemented a root-seeking routine to find the value of d that provided the required impedance value K and the angle ϕ for each impedance inverter.

7) Finally, the length of the jth resonator formed by the jth and $(j+1)$th strips is given by

$$l_j = \frac{\lambda_{go}}{2\pi}\left[\pi - \frac{1}{2}(\phi_j + \phi_{j+1})\right] \tag{11}$$

III. Design and Measurement

The method described above was applied to the design of E-plane filters for use in various frequency regions, ranging from Ka (26.5–40 GHz) to D (110–175 GHz) band. In this paper, we discuss three examples, one each for D-, W-, and U-bands. Note that the procedure is valid for E-plane filters of bilateral, and unilateral, and metal-only construction.

TABLE I
D-Band Filter Design

Ripple:	0.10 dB
Lower Band-Edge Frequency:	139.0 GHz
Upper Band-Edge Frequency:	151.0 GHz
Lower Rejection :	20.0 dB at 132.0 GHz
Upper Rejection :	20.0 dB at 160.0 GHz
Relative Dielectric Consistant:	2.1
Substrate Thickness/Inches:	0.003
Waveguide Width/Inches:	0.065
No. of Resonators:	5
Strips $d_1 = d_6 = 1.25$, $d_2 = d_5 = 13.25$, $d_3 = d_4 = 17$ mils	
Resonators $l_1 = l_5 = 34.93$, $l_2 = l_4 = 35.39$, $l_3 = 35.40$ mils	

TABLE II
D-Band Filter Response

Frequency (GHz)	Return Loss (db)	Insertion (db)
130.000	0.000	51.480
131.000	0.000	47.463
132.000	0.001	43.125
133.000	0.001	38.385
134.000	0.003	33.160
135.000	0.009	27.267
136.000	0.037	20.486
137.000	0.242	12.499
138.000	2.292	3.797
139.000	17.047	0.054
140.000	23.726	0.001
141.000	53.904	0.015
142.000	22.584	0.015
143.000	23.270	0.014
144.000	59.235	0.007
145.000	22.635	0.018
146.000	19.720	0.040
147.000	23.958	0.010
148.000	30.072	0.003
149.000	18.466	0.058
150.000	20.014	0.038
151.000	15.733	0.105
152.000	3.823	2.310
153.000	0.887	7.325
154.000	0.250	12.550
155.000	0.087	17.086
156.000	0.039	20.946
157.000	0.020	24.286
158.000	0.012	27.198
159.000	0.008	29.765
160.000	0.007	32.038

Table I shows specifications for a D-band filter and the initial guess of dimensions for the strips (d_j) and resonators (l_j) derived by procedures 1) through 7) described above. When these values are used in the analysis portion of the CAD program, the response is as shown in Table II. Since these results satisfy the specifications, no optimization was required.

A bilateral D-band filter (Table I) was fabricated and tested. A 3-mil-thick cuflon substrate is used for this filter. Fig. 4 shows the measured insertion loss of this filter. Since two sweep generators were used for this measurement, the two printouts are placed side by side to generate Fig. 4. The measured results indicate that the entire passband is shifted upward by about 3.5 GHz. However, this shift constitutes only about 2.4 percent of the center frequency. Such a shift is caused by the thickness of the strip metallization and by the grooves holding the E-plane substrate. The groove dimension is 5 mils wide by 3 mils deep, and Fig. 5 is a photograph of the D-band filter.

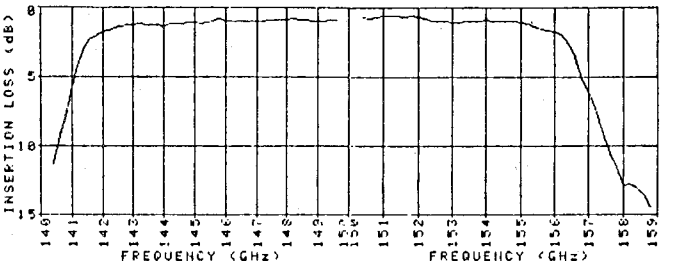

Fig. 4. Measured characteristics of a *D*-band bilateral filter on a cuflon substrate.

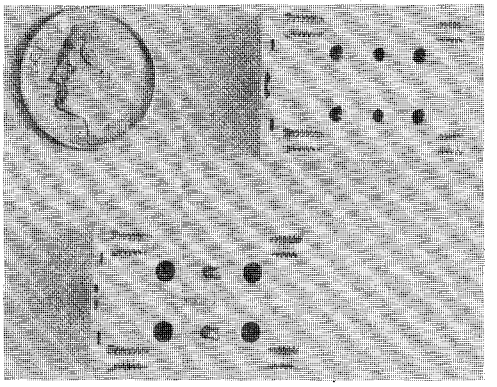

Fig. 5. Photograph of a *D*-band filter.

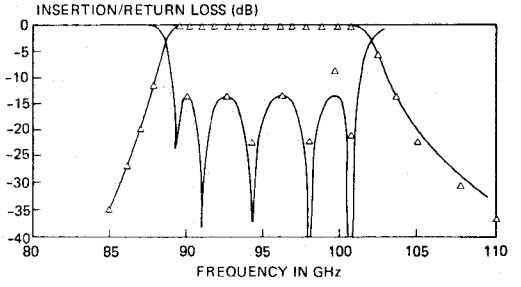

Fig. 6. *W*-band bilateral filter on a 5-mil-thick RT duroid. $d_1 = d_6 = 1.25, d_2 = d_5 = 15.25, d_3 = d_4 = 20.25$ mils, $l_1 = l_5 = 53.29, l_2 = l_4 = 54.02, l_3 = 54.05$ mils.

In Fig. 6, the predicted and measured insertion loss and return loss of a bilateral *W*-band filter fabricated on a 5-mil RT/Duroid substrate are given (measured data are indicated by (x)). Fig. 7 presents measured data for a unilateral, 7-resonator *U*-band filter with relative bandwidth exceeding 20 percent. The design specified the passband from 50 to 60 GHz. In the measurement, a *V*-band sweeper (50 to 75 GHz) was used via a tapered transition to the *U*-band setup.

IV. Conclusions

An efficient method for estimating the starting values of a broad-band *E*-plane filter was developed using a conventional direct-coupled filter and the exact equivalent circuit of an *E*-plane inductive strip. Compared to our original CAD procedure, this modified version's CPU time is reduced by a factor of 30. Excellent agreement with exact analysis and measurements has been obtained for filter designs of up to 160 GHz. Performance of these filters, particularly those at *D*-band, is unmatched to date.

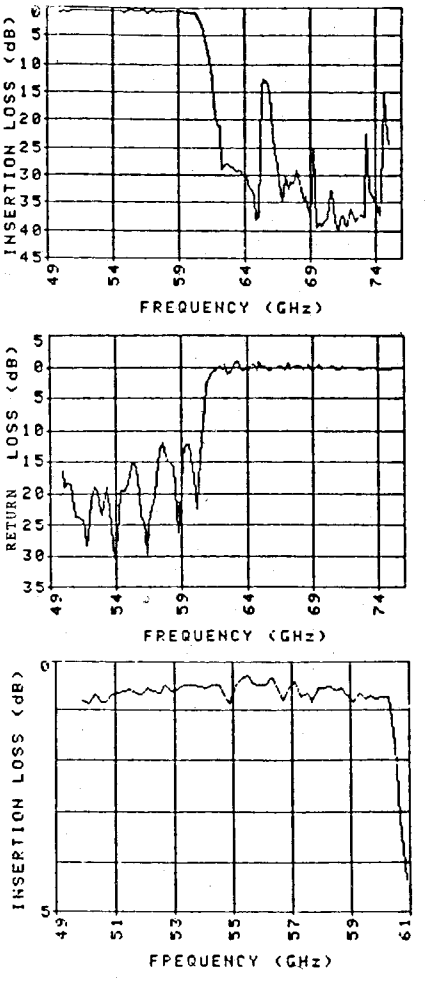

Fig. 7. Measured responses of a *U*-band, unilateral 7-resonator filter. $d_1 = d_8 = 1.5, d_2 = d_7 - 20.25, d_3 = d_6 = 29.75, d_4 = d_5 = 32.25$ mils, $l_1 = l_7 = 85.73, l_2 = l_6 = 85.53, l_3 = l_5 = 85.25, l_4 = 85.20$ mils.

References

[1] Y. Konishi and K. Uenakada, "The design of a bandpass filter with inductive strip-planar circuit mounted in waveguide," *IEEE Trans. Microwave Theory Tech.*, vol. MTT-22, pp. 1209–1216, 1974.

[2] Y. Tajima and Y. Sawayama, "Design and analysis of a waveguide-sandwich microwave filter," *IEEE Trans. Microwave Theory Tech.*, vol. MTT-22, pp. 839–841, 1974.

[3] P. Meier, "Integrated fin-line millimeter components," *IEEE Trans. Microwave Theory Tech.*, vol. MTT-22, pp. 1209–1216, 1974.

[4] F. Arndt *et al.*, "Theory and design of low-insertion loss fin-line filters," *IEEE Trans. Microwave Theory Tech.*, vol. MTT-30, pp. 155–162, 1982.

[5] A. M. K. Saad and K. Schunemann, "Design and performance of fin-line bandpass filters," in *Proc. 10th Eur. Microwave Conf.*, (Warsaw), Sept. 1980, pp. 397–401

[6] Y. C. Shih, T. Itoh, and L. Q. Bui, "Computer-aided design of millimeter-wave *E*-plane filters," *IEEE Trans. Microwave Theory Tech.*, vol. MTT-31, pp. 135–142, 1983.

[7] Subroutine ZXMIN, ZXSSQ of IMSL Library.

[8] R. Levey, "Theory of direct-coupled cavity filters," *IEEE Trans. Microwave Theory Tech.*, vol. MTT-15, pp. 340–348, 1967.

[9] L. Young, "Direct-coupled cavity filters for wide and narrow bandwidths," *IEEE Trans. Microwave Theory Tech.*, vol. MTT-11, pp. 162–178, 1963.

[10] J. D. Rhodes, "Microwave circuit realizations," in *Microwave Solid State Devices and Applications*, D. V. Morgan and M. J. Haves, Eds. England: Peregrinus, 1980, pp. 49–57.

[11] C. F. Vanblaricum, Jr. and R. Mittra, "A modified residue-calculus technique for solving a class of boundary value problems—Part II: Waveguide phase arrays, modulated surfaces, and diffraction gratings," *IEEE Trans. Microwave Theory Tech.*, vol. MTT-17, pp. 310–319, 1969.